doi.org/10.36721/PJPS/2026.40.16650.1

Predictive potential of pretreatment pepsinogen and platelet-to-lymphocyte ratios for postoperatively confirmed perineural invasion in gastric cancer patients receiving paclitaxel-based chemotherapy followed by radical surgery

Yongliang Li[#,*], Xi Lin[#], Guofeng Lin and Feiteng Gu
Department of Gastrointestinal Surgery, Affiliated Hospital of Putian University, Putian, Fujian, 351100, China

Abstract: **Background**: Perineural invasion (PNI) predicts poor prognosis in gastric cancer (GC) but lacks convenient preoperative biomarkers. **Objectives**: To investigate the predictive value of pretreatment platelet-to-lymphocyte ratio (PLR) and pepsinogen ratio (PGR) for postoperatively confirmed PNI in GC patients receiving paclitaxel-based chemotherapy followed by radical surgery. **Methods**: We retrospectively analyzed the medical records and clinical data of 110 patients with gastric cancer who underwent radical resection after paclitaxel-based neoadjuvant chemotherapy (from June 2023 to June 2025). Patients were divided into PNI-positive (n=45) and PNI-negative (n=65) groups. LASSO and logistic regression identified independent predictors. ROC curves, calibration, DCA and Spearman correlation were performed. **Results**: Of the 110 patients, 45 were PNI-positive and 65 were PNI-negative. Compared with the PNI-negative group, the PNI-positive group had significantly higher proportions of elevated CA19-9, increased tumor thickness, elevated PLR, diffuse/mixed Lauren type, Borrmann type III, T3-4 invasion, lymph node metastasis, TNM stage II/III and tumor diameter ≥5 cm, but significantly lower PGR (all $P<0.05$). LASSO identified nine non-zero coefficient indicators: CA19-9, tumor thickness, PLR, PGR, Lauren classification, Borrmann type III, tumor invasion, lymph node metastasis and TNM stage. Elevated PLR and advanced TNM stage were risk factors, while elevated PGR was a protective factor. ROC analysis showed apparent AUCs for PLR, TNM stage, PGR and the combined model of 0.786, 0.834, 0.807 and 0.851, respectively. PGR was negatively correlated with PNI ($r = -0.749$), whereas PLR ($r = 0.698$) and TNM stage ($r = 0.751$) were positively correlated. **Conclusion**: Pretreatment PLR and PGR show moderate predictive value for PNI in GC patients after paclitaxel chemotherapy, with slightly improved combined performance when TNM stage is added. External validation is required before clinical application.

Keywords: Gastric cancer; Nerve invasion; Paclitaxel chemotherapy; Platelet-to-lymphocyte ratio; Pepsinogen; Postoperative pathology

Submitted on 21-04-2026 – Revised on 17-06-2026 – Accepted on 30-06-2026

INTRODUCTION

The development of gastric cancer (GC) results from the interaction of environmental factors such as smoking and high-salt diet with microbial factors including Helicobacter pylori infection and it is the fifth most common malignancy worldwide (Özcan and Çarkmant, 2024). Currently, chemotherapy combined with surgery is commonly used to treat GC. Among chemotherapeutic agents, albumin-bound paclitaxel (nab-paclitaxel, nab-PTX) is a nanoparticle formulation that achieves higher tumor drug concentrations and reduces systemic toxicity (Wang et al., 2025), demonstrating significant value in GC management. However, some patients still experience poor prognosis even after chemotherapy (Cao *et al*., 2024), suggesting the presence of other key factors affecting treatment response and prognosis.

Perineural invasion (PNI) is a prognostic factor for GC, accounting for up to 40.5% of the total pathological findings in GC patients after surgery (Li *et al*., 2022) and it is an important cause of local recurrence and shortened survival. Therefore, effective identification of high-risk populations for PNI is crucial for developing individualized adjuvant treatment strategies and improving patient survival. However, there is currently a lack of convenient and reliable biomarkers to predict the risk of PNI in surgical specimens after paclitaxel chemotherapy.

The inflammatory immune response in tumor patients affects the occurrence and development of cancer to some extent (Sohrab *et al*., 2023). The platelet-to-lymphocyte ratio (PLR) can assess the immune and inflammatory status of patients with various malignant tumors. In a meta-analysis, high PLR levels were confirmed to be associated with poor progression-free survival (HR=1.52) and overall survival (HR=1.57) ($P<0.01$) (Tan *et al*., 2024). In addition, the pepsinogen ratio (PGR) is an indicator of gastric mucosal health and activity. Changes in its serum level reflect alterations in gastric function and

*Corresponding author: e-mail: lylfjpt@126.com
#These authors contributed equally and are the co-first authors.

mucosal inflammation and it is a marker for assessing atrophic gastritis and early GC (Nasier-Hussain *et al*., 2025). However, PLR and PGR are associated with inflammatory status and the gastric mucosal microenvironment, respectively; whether they can predict PNI occurrence in the pathological tissues of GC patients after paclitaxel chemotherapy has not been systematically studied. Furthermore, existing studies have mostly focused on baseline PNI status, leaving a gap in research on the use of peripheral blood indicators to predict PNI risk at final surgical pathology during the "post-chemotherapy, pre-surgery" time window.

Based on this, this study retrospectively collected clinical data from GC patients who received paclitaxel-based neoadjuvant chemotherapy followed by radical surgery, aiming to explore the association between pretreatment serum PGR and peripheral blood PLR levels and postoperatively confirmed PNI status, thereby clarifying the predictive value of these indicators for PNI and providing a reference for early clinical identification of high-risk patients and the development of individualized treatment strategies.

MATERIALS AND METHODS

Study subjects

Study setting and patient selection: This retrospective study was conducted at the Department of Gastrointestinal Surgery, Affiliated Hospital of Putian University, a tertiary teaching hospital in Fujian, China. The medical records of patients with gastric cancer who were treated between June 2023 and June 2025 were systematically reviewed. Eligible patients were identified through the hospital's electronic medical record (EMR) system using International Classification of Diseases, 10th Revision (ICD-10) codes for gastric cancer (C16.0–C16.9) and procedure codes for radical gastrectomy. A total of 186 patients were initially screened. Of these, 76 were excluded for the following reasons: 31 did not receive paclitaxel-based neoadjuvant chemotherapy, 18 had missing key clinical data (PGI/PGII, PLR, or TNM staging), 12 had ECOG performance status scores that did not meet the inclusion criteria, 8 were lost to follow-up or had a survival period <12 weeks and 7 had concurrent primary malignancies or severe hematopoietic disorders. After exclusions, 110 patients who met all inclusion criteria were consecutively enrolled. The patient selection and data collection period extended from June 2023 to June 2025. Clinical, laboratory and pathological data were extracted from the EMR system by two independent trained research assistants, with discrepancies resolved by consensus. The study was approved by the institutional ethics committee (NO. 2025698) and informed consent was waived due to the retrospective anonymous data analysis.

Inclusion criteria were: (1) preoperative pathological examination confirmed gastric cancer; (2) CT or MRI showed at least one measurable lesion; (3) Eastern Cooperative Oncology Group (ECOG) performance status score qualified; (4) treatment regimen of paclitaxel chemotherapy combined with radical gastrectomy for gastric cancer; (5) survival period ≥12 weeks; (6) no missing clinical data.

Exclusion criteria were: (1) accompanied by primary diseases of important organs or the hematopoietic system; (2) presence of severe hematopoietic dysfunction or blood-related diseases; (3) comatose or with mental or psychological diseases; (4) unable to perform independent activities; (5) presence of severe malnutrition.

Sample size calculation (Park et al., 2023): The sample size was determined by the events per variable (EPV) method. With EPV=10 as the standard for sample size estimation, a total of 9 predictive factors were included, requiring n=90. Accounting for 20% loss to follow-up, a final sample size of 110 cases was determined.

Patient selection process: A total of 186 patients with gastric cancer who were assessed for eligibility between June 2023 and June 2025 were initially screened. Of these, 76 patients were excluded for the following reasons: 31 did not receive paclitaxel-based neoadjuvant chemotherapy, 18 had missing key clinical data (including PGI/PGII, PLR, or TNM staging information), 12 had ECOG performance status scores that did not meet the inclusion criteria, 8 were lost to follow-up or had a survival period <12 weeks and 7 were excluded due to concurrent primary malignancies or severe hematopoietic disorders. After exclusion, 110 patients were ultimately included in the final analysis (Fig.1).

Methods

Serological indicator detection

Peripheral blood test data from before treatment were retrieved from the medical record system. Fasting venous blood (2 mL) was collected into a routine blood collection tube and mixed thoroughly with anticoagulant. Platelet and lymphocyte counts were measured using a Maikaidi BT-71 automated hematology analyzer and the platelet-to-lymphocyte ratio (PLR) was calculated. Additionally, 4 mL of venous blood was collected into a coagulation tube, centrifuged at 3500 r/min for 10 minutes and the upper serum layer was collected. The levels of carcinoembryonic antigen (CEA), carbohydrate antigen 125 (CA125), alpha-fetoprotein (AFP) and carbohydrate antigen 19-9 (CA19-9) were measured using a Lanlike LK5100 electrochemiluminescence immunoassay analyzer. The levels of pepsinogen I (PGI) and pepsinogen II (PGII) were measured using a fully automated biochemical analyzer (Hitachi 7600) and a pepsinogen detection kit (Beijing Jiuqiang Biotechnology Co., Ltd.) and the PGR value was calculated as PGR = PGI ÷ PGII(Nasier-Hussain *et al*.,2025).

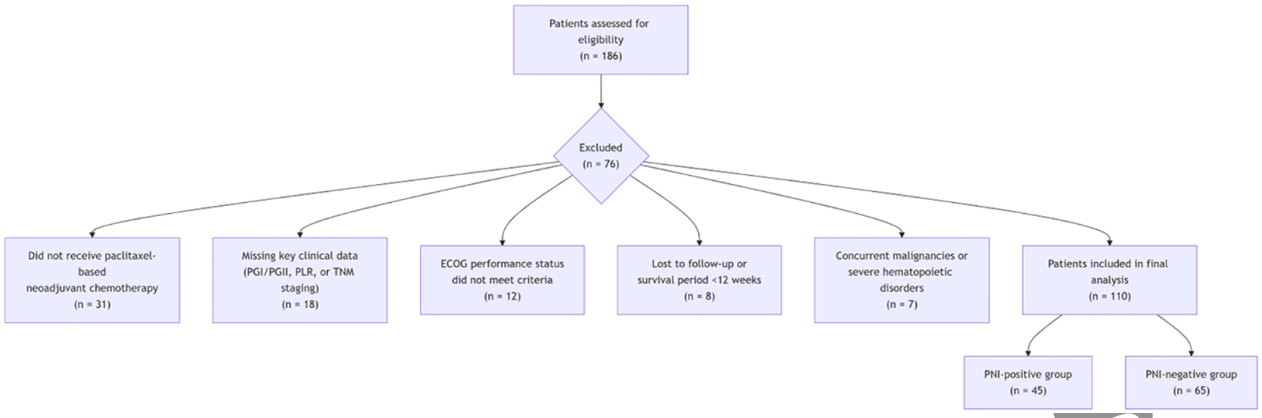


Fig. 1: Patient selection flow diagram. A total of 186 patients were initially assessed for eligibility. After excluding 76 patients for the reasons listed, 110 patients were included in the final analysis and divided into PNI-positive (n = 45) and PNI-negative (n = 65) groups based on postoperative pathological diagnosis.

Treatment regimen and grouping

Chemotherapy and surgical records were extracted from the medical record system. Neoadjuvant chemotherapy was administered using nab-PTX (Qilu Pharmaceutical, National Drug Approval Number H20193309). On the first day of treatment, the dosage was 260 mg/m² and patients received albumin-bound paclitaxel infusion. One treatment cycle lasted 21 days and treatment was continued for 6 cycles, followed by standard radical gastrectomy (D2 lymph node dissection). The treatment regimen and surgical approach were uniformly formulated by a multidisciplinary team, ensuring consistency.

Grouping: Based on postoperative pathological diagnosis of perineural invasion (PNI), patients were divided into a PNI-negative group (65 cases) and a PNI-positive group (45 cases).

Immunohistochemical staining and PNI determination

Archived paraffin-embedded tissue specimens were retrieved and representative sections from both groups were selected. AE1/AE3 antibody (Abcam, ab215202, 1:100) was used to label cancer cells and S100 antibody (Abcam, ab4066, 1:100) was used to label nerve tissue for dual immunohistochemical staining. Sections were subjected to antigen retrieval at 95°C for 15 minutes, then incubated with S100 antibody at 4°C for 16 hours, detected using a biotinylated antibody combined with 5-bromo-4-chloro-3-indolyl phosphate/nitroblue tetrazolium chromogenic system. After antigen retrieval, sections were incubated with AE1/AE3 antibody at 25°C for 2 hours and the reaction was detected using a catalase/AEC system (amine system reagents purchased from Shanghai Chunyou Biotechnology)(Chen *et al*.,2022). The criterion for PNI positivity was: under light microscopy, cancer cells invading any of the epineurium, perineurium, or endoneurium of nerve fibers, or cancer cells encircling ≥33% of the nerve circumference, with immunohistochemical staining showing S100-positive expression in nerve bundles (Liebig *et al*.,2009).

All sections were independently evaluated by two senior pathologists blinded to patient clinical information; disagreements were resolved through discussion. The inter-observer agreement Kappa value was 0.86 (95% CI: 0.79–0.93), indicating excellent agreement.

Data collection

The following clinical and pathological data were extracted from the medical record system: age, sex, AFP, CEA, CA125, CA19-9, tumor thickness, Lauren and Borrmann classifications, PGI, PGII, PGR, tumor invasion depth, lymph node metastasis, tumor diameter, positive tumor stump and TNM stage.

Statistical analysis

SPSS 27.0 and R software (4.2.0) were used for statistical analysis. Continuous data were expressed as mean±SD and analyzed using t-tests; categorical data were expressed as [n(%)] and analyzed using χ^2 tests or Fisher's exact test. $P<0.05$ was considered statistically significant. Sample size was estimated based on the EPV≥10 principle (9 predictors required 90 cases; accounting for 20% loss to follow-up, 110 cases were ultimately included). After univariate analysis, variance inflation factor (VIF) was calculated, revealing severe multicollinearity for Borrmann classification (VIF=12.359) and tumor invasion depth (VIF=15.416) (VIF>10, tolerance<0.1). To avoid model instability, LASSO regression was used as the sole variable selection strategy (10-fold cross-validation, λ=0.140), identifying 9 non-zero coefficients (CA19-9, tumor thickness, PLR, PGR, Lauren classification, Borrmann classification, tumor invasion depth, lymph node metastasis and TNM stage). These were then included in a multivariate logistic regression (forward stepwise method) to identify independent predictors (TNM stage and PLR as risk factors, PGR as a protective factor) and a combined prediction model was constructed. ROC curves were used to evaluate predictive performance, with optimal cut-off

values determined by the maximum Youden index and corresponding sensitivity and specificity were calculated. Bootstrap resampling (1000 iterations) was used to calculate the C-index (0.877, 95% CI: 0.715–0.924) and plot calibration curves (Hosmer-Lemeshow test: χ^2=3.927, P=0.283). Decision curve analysis (DCA) was used to assess clinical net benefit and Spearman rank correlation analysis was used to assess correlations with PNI.

It should be noted that LASSO regression was chosen for variable selection for the following reasons: (1) a relatively large number of candidate variables (23) with limited sample size (110), posing a risk of overfitting; (2) collinearity diagnostics indicated severe multicollinearity for Borrmann classification and tumor invasion depth (VIF>10), which would destabilize coefficient estimation in ordinary logistic regression; (3) LASSO regression simultaneously performs variable selection and coefficient shrinkage via L1 penalty and the λ.1se criterion prioritizes sparser models to improve generalizability. Based on LASSO selection, multivariate logistic regression was used to construct the prediction model, outputting ORs and 95% CIs to balance predictive performance and clinical interpretability. Model performance was evaluated using ROC curves (discrimination), calibration curves and the Hosmer-Lemeshow test (calibration) and DCA (clinical utility), with internal validation via bootstrap resampling (1000 iterations). This combination of methods is recommended for clinical prediction model studies with small to moderate sample sizes. Furthermore, this is a single-center retrospective study; the AUCs reflect apparent performance, with potential optimism bias and the model's external generalizability requires validation in independent external cohorts. The results should be considered preliminary findings. Due to the retrospective anonymous data analysis, informed consent was waived.

Several measures were implemented to minimize potential biases in this retrospective study.
Selection bias: To reduce selection bias, we consecutively enrolled all patients who met the pre-specified inclusion and exclusion criteria during the study period, rather than using a convenience sample. The eligibility criteria were clearly defined before data extraction and all potentially eligible patients were identified through a systematic electronic medical record search using ICD-10 codes, which minimized the risk of selective inclusion. The patient selection process and reasons for exclusion are transparently reported in the flow diagram.

Information/measurement bias: To minimize information bias, clinical, laboratory and pathological data were extracted from the electronic medical record system by two independent trained research assistants using a standardized data collection form. Discrepancies were resolved through discussion with a third investigator. Laboratory parameters (including PLR and PGR) were measured using standardized automated analyzers with established quality control protocols. Pathological evaluation of PNI was performed by two senior pathologists who were blinded to all clinical information, including treatment allocation and patient outcomes; inter-observer agreement was excellent (Kappa = 0.86, 95% CI: 0.79–0.93). All data were collected prospectively into the medical record system during routine clinical care and the investigators performing the statistical analyses were blinded to the grouping status during the initial data cleaning phase.

Confounding: To address potential confounding, we adopted a two-step analytical strategy. First, LASSO regression was used for variable selection to identify the most relevant predictors among 23 candidate variables, which simultaneously reduces the risk of overfitting and controls for multicollinearity. Second, multivariate logistic regression was performed to adjust for potential confounders, including clinically and statistically relevant variables. The variance inflation factor was calculated to detect multicollinearity among predictors and variables with VIF > 10 were handled appropriately. The calibration curve and Hosmer-Lemeshow test (χ^2 = 3.927, P = 0.283) confirmed that the final model was well calibrated.
Bias from exclusion of patients with missing data: To minimize bias arising from missing data, we explicitly report in the patient flow diagram the number of patients excluded due to missing clinical data (n = 18). The specific variables with missing data included PGI/PGII, PLR and TNM staging information. Patients with missing data on key variables were excluded from the analysis, as the missingness was considered non-random and directly related to the availability of complete medical records. Importantly, the proportion of excluded patients (18/186, 9.7%) was relatively small and unlikely to substantially affect the overall results. Furthermore, the sample size was calculated a priori using the EPV method (EPV ≥ 10), ensuring adequate statistical power for the planned analyses. All exclusion criteria and reasons for exclusion are transparently described to allow readers to assess the potential impact of missing data on the study findings.

Handling of missing data: In this retrospective study, complete-case analysis was adopted. As specified in the inclusion criteria (item 6: "no missing clinical data"), only patients with complete data for all key variables of interest were included in the final analysis. A total of 18 potentially eligible patients were excluded from the study because of missing clinical data. The specific variables with missing data were as follows: pepsinogen I/II (PGI/PGII) or the derived pepsinogen ratio (PGR) was missing in 8 patients; platelet-to-lymphocyte ratio (PLR) could not be calculated due to incomplete blood count results in 5 patients; and TNM staging information was incomplete or unavailable in the medical records of 5

Article in Press

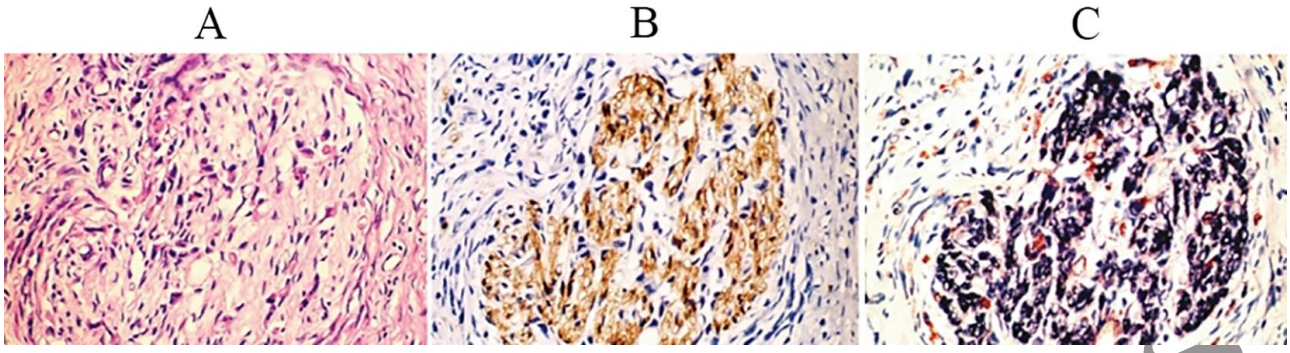


Fig. 2: Representative immunohistochemical staining for perineural invasion (PNI) in gastric cancer tissue. (A) Hematoxylin and eosin (H&E) staining showing a nerve bundle surrounded by diffuse-type gastric cancer cells (original magnification ×400); (B) S100 immunohistochemical staining marking the nerve in brown (arrow), with cancer cells appearing faintly counterstained (original magnification ×400); (C) Double immunohistochemical staining with S100 (nerve, dark blue) and AE1/AE3 (cancer cells, red) showing a cancer cell cluster (red) invading around a nerve fiber (dark blue) (original magnification ×400). The double staining allows rapid visual assessment of cancer-nerve interaction. Scale bar = 50 μm.

patients.

No other important variables (including CA19-9, tumor thickness, Lauren classification, Borrmann classification, tumor invasion depth, lymph node metastasis, tumor diameter, or positive tumor stump) had missing values in the remaining screened patients. Because the proportion of patients with missing data was relatively small (18/186, 9.7%) and because the missingness was primarily attributable to incomplete medical records rather than patient characteristics, we did not perform imputation for missing values. Instead, these patients were excluded from the analysis to avoid the potential bias that could be introduced by imputation methods. This complete-case approach ensured consistency across all analyses and preserved the integrity of the dataset. All exclusion decisions were made before any outcome analysis and the exclusion process is transparently reported in the patient selection flow diagram.

RESULTS

Immunohistochemical staining results of PNI

H&E staining (Fig. 2A) revealed a nerve in diffuse GC. S100 staining (Fig. 2B) marked the nerve (shown as brown), while cancer cells were blurred. After double staining (Fig. 2C), the nerve appeared deep blue and scattered cancer cells appeared red, allowing for rapid assessment of the extent of invasion around the nerve.

Comparison of clinical data

A total of 110 GC patients receiving paclitaxel-based chemotherapy were included. PNI status was determined from postoperative pathological specimens. Based on PNI occurrence, they were assigned to a PNI-negative group (65 cases) and a PNI-positive group (45 cases). Compared with the PNI-negative group, the PNI-positive group had significantly higher proportions of elevated CA19-9, increased tumor thickness, elevated PLR, diffuse/mixed Lauren type, Borrmann type III, T3-4 invasion, lymph node metastasis, TNM stage II/III and tumor diameter ≥5 cm, but significantly lower PGR (all $P<0.05$), as shown in table 1.

LASSO regression model

A LASSO regression model was established by screening the 23 variables in table 1. The results showed that when the optimal λ (λ = 0.140, i.e., lambda.1se) was reached, 9 indicators with non-zero coefficients were selected, namely CA19-9, tumor thickness, PLR, PGR, Lauren classification, Borrmann type III, tumor invasion depth, lymph node metastasis and TNM stage, as shown in figure 3.

Factors affecting PNI occurrence in GC patients undergoing paclitaxel chemotherapy

PNI occurrence in GC patients after paclitaxel chemotherapy was used as the dependent variable and factors with $P<0.05$ from univariate analysis were included as independent variables. Univariate analysis followed by collinearity analysis revealed severe collinearity (VIF > 10, tolerance < 0.1) among the factors with P <; these factors were excluded. TNM stage (OR=1.783, 95% CI: 1.462–2.104) and PLR (OR=1.913, 95% CI: 1.667–2.159) were independent risk factors for PNI ($P<0.05$); PGR (OR=0.532, 95% CI: 0.207–0.657) was an independent protective factor ($P<0.05$). A combined prediction model was constructed with the formula: $Y = -2.594 + 1.636 \times (\text{TNM stage}) + 1.911 \times (\text{PLR}) - 1.364 \times (\text{PGR})$. See tables 2 and 3 and figure 4.

Predictive power of ROC analysis of influencing factors

ROC analysis (Fig. 5) showed that the apparent AUCs for PGR, PLR and TNM stage were 0.807, 0.786 and 0.834, respectively, while the combined model AUC was 0.851, indicating moderate to good predictive performance for each indicator and the combined model.

Article in Press

Table 1: Comparison of clinical data between the PNI positive group and the PNI negative group.

Indicators		PNI positive group (n=45)	PNI negative group (n=65)	t/χ^2	*P*
Age (years)		64.28±7.65	66.03±5.19	1.430	0.155
Gender [n(%)]	Male	32 (71.11)	37 (56.92)	2.289	0.130
	Female	13 (28.89)	28 (43.08)		
AFP ($\bar{x}$±s, ng/ml)		2.24±0.65	2.15±0.61	0.741	0.461
CEA ($\bar{x}$±s, ng/ml)		55.14±8.71	53.08±7.96	1.284	0.202
CA125 ($\bar{x}$±s,U/ml)		121.58±26.37	119.08±24.18	0.514	0.609
CA19-9 ($\bar{x}$±s, U/ml)		11.76±3.65	6.88±2.05	8.943	<0.001
Tumor thickness ($\bar{x}$±s, mm)		20.25±5.06	14.17±4.25	6.820	<0.001
Lauren classification [n(%)]	Intestinal type	14 (31.11)	49 (75.38)	21.535	<0.001
	Diffuse type	14 (31.11)	6 (9.23)		
	Mixed type	17 (37.78)	10 (15.38)		
PGI ($\bar{x}$±s,ng/ml)		54.24±12.63	56.38±11.25	0.933	0.353
PGII ($\bar{x}$±s,ng/ml)		11.07±2.14	10.66±2.69	0.852	0.396
PGR ($\bar{x}$±s)		5.01±2.06	7.26±2.35	5.188	<0.001
PLR ($\bar{x}$±s)		158.06±51.32	132.58±49.36	2.619	0.010
Tumor invasion degree [n(%)]	T1~2	10 (22.22)	45 (69.23)	23.504	<0.001
	T3~4	35 (77.78)	20 (30.77)		
Lymph node metastasis [n(%)]	No	16 (35.56)	47 (72.31)	14.677	<0.001
	Yes	29 (64.44)	18 (27.69)		
TNM staging [n(%)]	I	2 (4.44)	38 (58.46)	35.197	<0.001
	II	14 (31.11)	13 (20.00)		
	III	29 (64.44)	14 (21.54)		
Smoking history	Yes	21 (46.67)	32 (49.23)	0.070	0.791
	No	24 (53.33)	33 (50.77)		
Alcohol consumption history	Yes	23 (51.11)	26 (40.00)	1.329	0.249
	No	22 (48.89)	39 (60.00)		
Hypertension	Yes	5 (11.11)	9 (13.85)	0.179	0.672
	No	40 (88.89)	56 (86.15)		
Diabetes	Yes	3 (6.67)	4 (6.15)	0.084	0.773
	No	42 (93.33)	61(93.84)		
Coronary heart disease	Yes	7 (15.56)	10 (15.38)	0.001	0.981
	No	38 (84.44)	55 (84.62)		
Tumor diameter	<5cm	17 (37.78)	40 (61.54)	6.013	0.014
	≥5cm	28 (62.22)	25 (38.46)		
Positive tumor stump [n(%)]	No	39 (86.67)	64 (98.46)	4.387	0.036
	Yes	6 (13.33)	1(1.54)		

Note: AFP, alpha-fetoprotein; CEA, carcinoembryonic antigen; CA125, carbohydrate antigen 125; CA19-9, carbohydrate antigen 19-9; PGI, pepsinogen I; PGII, pepsinogen II; PGR, pepsinogen ratio; PLR, platelet-to-lymphocyte ratio.

Article in Press

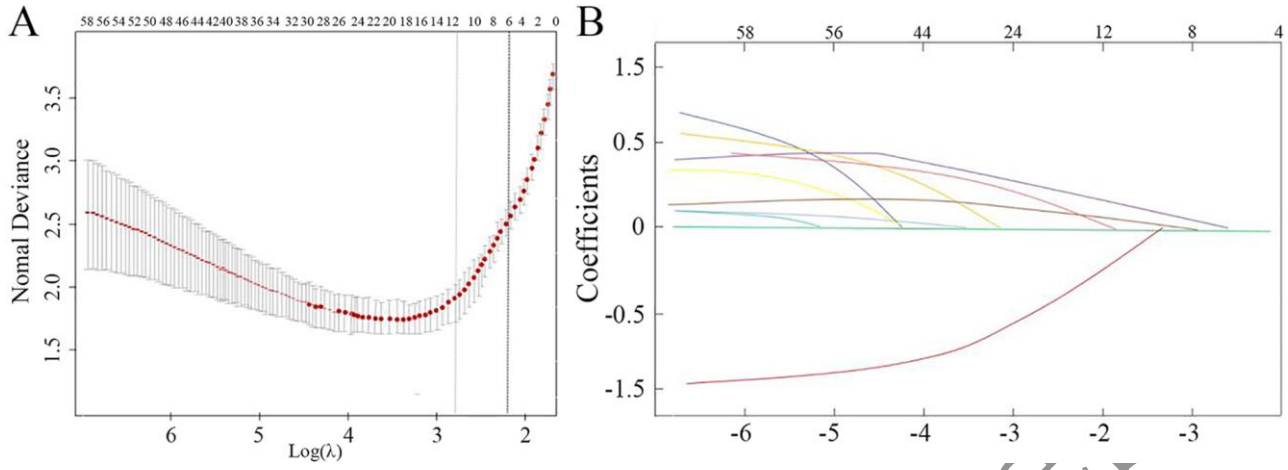


Fig. 3: LASSO regression for variable selection. (A) Cross-validation plot of the penalty term (λ). The x-axis shows log(λ) and the y-axis shows the binomial deviance (a measure of model fit). The left vertical dashed line represents the λ value that gives the minimum deviance (λ.min), while the right vertical dashed line represents λ.1se (λ = 0.140), the largest λ within one standard error of the minimum deviance. λ.1se was selected for the final model to balance predictive accuracy and model parsimony. The error bars represent ±1 SE from 10-fold cross-validation; (B) LASSO coefficient profiles for 23 clinical variables as a function of log(λ). Each colored line represents the coefficient trajectory of an individual variable. As the penalty (λ) increases, coefficients shrink toward zero. At the selected λ.1se (right vertical dashed line), 9 variables with non-zero coefficients were retained: CA19-9, tumor thickness, PLR, PGR, Lauren classification, Borrmann type III, tumor invasion depth, lymph node metastasis, and TNM stage. The number of variables with non-zero coefficients at each λ is shown at the top of the plot. Variable selection was performed on the derivation cohort (N=110). These selected variables were subsequently entered into multivariate logistic regression analysis.

Table 2: Univariate logistic regression analysis of factors influencing PNI in GC-paclitaxel chemotherapy.

Factors	Assignment		*β*	*SE*	*Wald* χ^2	*P*	*OR (95%CI)*
CA19-9	X1	Substituting real values	0.187	0.097	3.718	0.053	1.206(0.835-1.577)
Tumor thickness	X2	Substituting real values	0.753	0.279	7.285	0.007	2.125(1.891-2.359)
Lauren classification	X3	Intestinal type = 1, Diffuse type = 2, Mixed type = 3	0.521	0.212	6.041	0.014	1.683(1.337-2.029)
Borrmann classification	X4	I = 1, II = 2, III = 3, IV = 4	–0.664	0.237	7.895	0.005	0.514(0.194-0.834)
PGR	X5	Substituting real values	–0.698	0.307	5.185	0.023	0.497(0.179-0.815)
PLR	X6	Substituting real values	1.104	0.556	3.942	0.047	3.018(2.804-3.232)
Tumor invasion extent	X7	T1~2 = 1, T3~4 = 2	0.557	0.265	4.418	0.036	1.746(1.407-2.085
Lymph node metastasis	X8	Present = 1, Absent = 0	0.751	0.344	4.768	0.029	2.120(1.893-2.347)
TNM staging	X9	I=1, II=2, III=3	0.526	0.222	5.613	0.018	1.692(1.344-2.040)

Table 3: Collinearity analysis.

Factors	*VIF*	Tolerance
CA19-9	1.124	0.890
Tumor thickness	1.057	0.946
Lauren classification	1.285	0.778
Borrmann classification	12.359	0.081
PGR	1.186	0.843
PLR	1.217	0.821
Tumor invasion extent	15.416	0.065
Lymph node metastasis	11.873	0.084
TNM staging	8.942	0.112

Note: VIF > 10 or tolerance < 0.1 indicates severe multicollinearity. Borrmann classification, tumor invasion depth and lymph node metastasis exceeded this threshold.

Article in Press

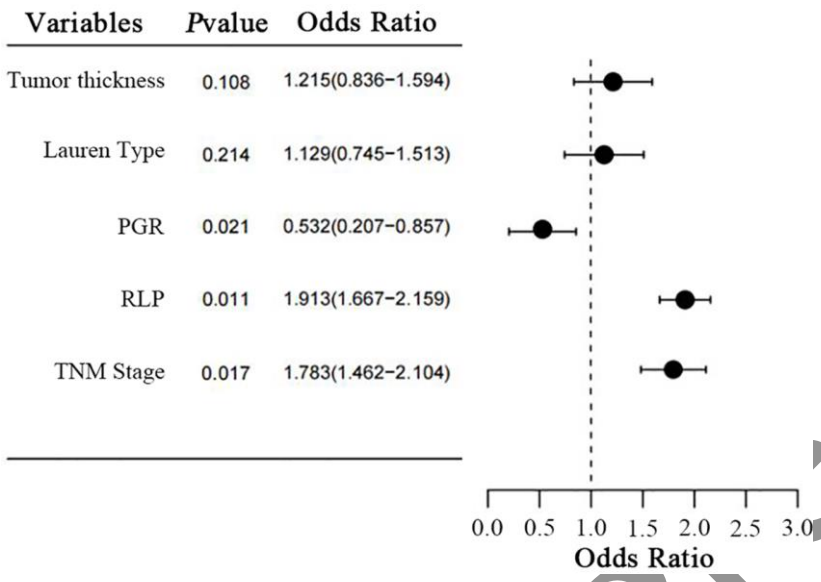


Fig. 4: Multivariate logistic regression analysis of independent factors associated with PNI. Forest plot displaying the odds ratios (ORs) with 95% confidence intervals (CIs) for the three independent predictors of PNI identified by the multivariable model. After adjustment for potential confounders, elevated PLR (OR = 1.913, 95% CI: 1.667–2.159, P < 0.001) and advanced TNM stage (OR = 1.783, 95% CI: 1.462–2.104, P < 0.001) were independent risk factors for PNI, while elevated PGR was an independent protective factor (OR = 0.532, 95% CI: 0.207–0.657, P = 0.004). The forest plot uses a logarithmic scale for the x-axis (OR). The dashed vertical line at OR = 1 represents no effect; variables to the right indicate increased risk, while variables to the left indicate decreased risk. Error bars represent 95% CIs. Analysis was based on the derivation cohort (N=110). OR, odds ratio; CI, confidence interval; PLR, platelet-to-lymphocyte ratio; PGR, pepsinogen ratio.

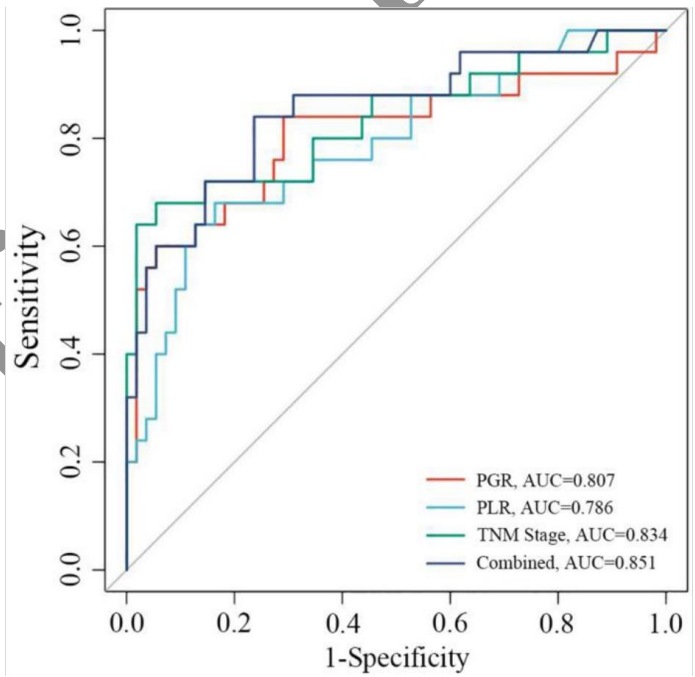


Fig. 5: Receiver operating characteristic (ROC) curves for predicting PNI in the derivation cohort (N=110). The apparent areas under the curve (AUCs) were 0.786 (95% CI: 0.702–0.870) for PLR, 0.807 (95% CI: 0.727–0.887) for PGR, 0.834 (95% CI: 0.758–0.910) for TNM stage, and 0.851 (95% CI: 0.780–0.922) for the combined model. All performance metrics are apparent estimates based on the derivation cohort and require external validation. Shaded areas represent 95% confidence intervals (bootstrap with 1,000 resamples). The diagonal dashed line represents the reference line (AUC = 0.5).

Art in Press

Table 4: Optimal cut-off values and apparent performance of each indicator for predicting PNI.

Indicator	Optimal cut-off value	Sensitivity (%)	Specificity (%)	Youden index	Apparent AUC (95% CI)
PLR	≥145.37	72.5	74.8	0.473	0.786 (0.702–0.870)
PGR	≤6.12	78.1	71.5	0.496	0.807 (0.727–0.887)
TNM stage	≥II	81.3	76.9	0.582	0.834 (0.758–0.910)
Combined model	≥0.382	85.6	80.2	0.658	0.851 (0.780–0.922)

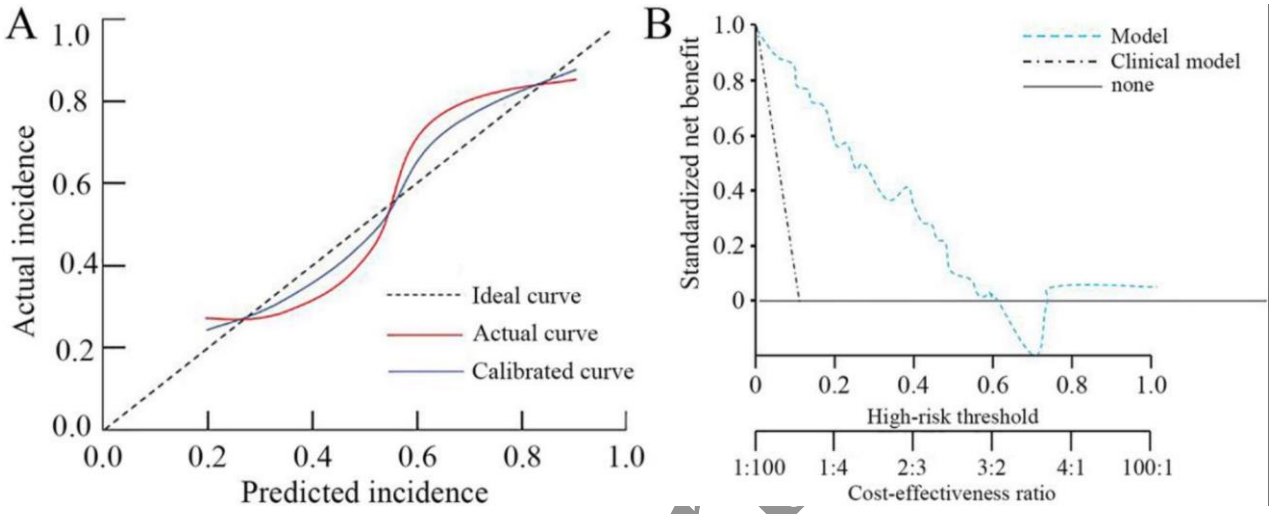


Fig. 6: Internal validation of the combined prediction model. (A) Calibration curve assessing the agreement between predicted probabilities and observed PNI outcomes in the derivation cohort. The diagonal dashed line represents perfect calibration (ideal prediction). The solid blue line represents the apparent performance of the model, with the solid red line representing the bias-corrected estimate after bootstrap resampling (1,000 iterations). The Hosmer-Lemeshow test yielded $\chi^2 = 3.927$ (P = 0.283), indicating no significant lack of fit; (B) Decision curve analysis (DCA) evaluating the clinical net benefit of the combined model across different threshold probabilities. The "Treat all" line assumes all patients receive intervention, while the "Treat none" line assumes no intervention. The combined model (blue line) shows positive net benefit across threshold probabilities ranging from 0% to 71% in the derivation cohort. Net benefit represents the trade-off between true positives (benefit) and false positives (harm). These results are based on the derivation cohort and require external validation.

Based on the maximum Youden index, the optimal cut-off values were: PGR ≤6.12 (sensitivity 78.1%, specificity 71.5%), PLR ≥145.37 (sensitivity 72.5%, specificity 74.8%), TNM stage ≥II (sensitivity 81.3%, specificity 76.9%) and combined model ≥0.382 (sensitivity 85.6%, specificity 80.2%), as shown in table 4. These cut-off values and performance metrics are based on the derivation cohort and represent apparent performance; confirmation in an independent validation cohort is required before clinical reference.

Validation of the combined prediction model

Calibration curve analysis (Fig. 6A) showed that the model closely approximated the ideal curve, indicating consistency between the combined model's predictions of PNI after paclitaxel chemotherapy in GC patients and the actual observed results in the study cohort (Hosmer-Lemeshow test: χ^2=3.927, P=0.283). Bootstrap resampling (1000 iterations) showed that the prediction model's C-index was 0.877 (95% CI: 0.715–0.924), indicating good discrimination and calibration. DCA curve analysis showed that the combined prediction model had a positive net benefit within the 0%–71% threshold range (Fig. 6B).

Correlation analysis of PGR, PLR and TNM stage with PNI occurrence

Spearman analysis showed that PGR was negatively correlated with PNI occurrence (r=−0.749, P=0.023); PLR was positively correlated with PNI occurrence (r=0.698, P=0.017); and TNM stage was positively correlated with PNI occurrence (r=0.751, P<0.001), as shown in figure 7.

DISCUSSION

PNI refers to the invasion of peripheral nerve fibers by GC cells and has been recognized as an important factor in assessing GC prognosis and treatment response (Huang *et al*., 2025). Relevant studies (Zhang *et al*., 2023) confirmed that, among GC patients, the 1- to 5-year survival rate was lower for those with positive vascular invasion/PNI than for those without (P<0.001).

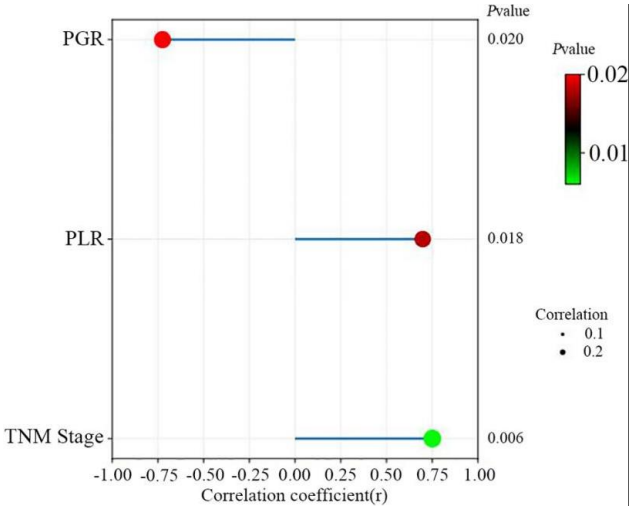


Fig. 7: Spearman correlation of PGR, PLR and TNM stage with PNI occurrence (derivation cohort, N=110). The lollipop chart displays the correlation coefficients (r) between each indicator and PNI. Horizontal bars extend from the reference line (r = 0) to the respective r value, with circles marking the endpoint. The length of the bar reflects the absolute strength of correlation. All three indicators showed statistically significant correlations with PNI: PGR (r = −0.749, P = 0.023), PLR (r = 0.698, P = 0.017) and TNM stage (r = 0.751, P < 0.001). PNI was treated as a binary variable (0 = negative, 1 = positive). These results are based on the derivation cohort and require external validation.

This suggests that PNI has important clinical significance in GC progression. Nano-albumin-bound paclitaxel (nab-PTX), as a special formulation of paclitaxel, does not contain polyethoxylated castor oil or dehydrated ethanol, which not only significantly reduces the risk of allergic reactions but also, due to its short infusion time and lack of routine premedication, is particularly suitable for patients with poor alcohol tolerance (Gangannapalle *et al*., 2023). Therefore, in clinical practice, nab-PTX has become an important option for GC chemotherapy. Effectively assessing PNI risk in GC patients receiving paclitaxel is thus of great significance. In addition to inhibiting tumor cell proliferation by stabilizing microtubules, paclitaxel can directly induce axonal degeneration and neurotoxicity in sensory neurons. A study using a human iPSC-derived sensory neuron model found that paclitaxel induces axonal damage through activation of the JNK/c-Jun pathway and the STE20 kinase family, while multi-kinase inhibition exerts neuroprotective effects (Petrova *et al*., 2026). The PNI positivity rate in this study was 40.91%, lower than the 57.1% reported in a relevant study (Chen *et al*., 2022), a difference that may partially reflect paclitaxel's inhibitory effect on PNI. However, both findings indicate that PNI is highly prevalent in GC. The PNI-positive group had higher rates of CA19-9 positivity, tumor thickness, PLR level, Lauren diffuse/mixed type, Borrmann type III, tumor invasion depth, lymph node metastasis, tumor diameter ≥5 cm, positive tumor stump and a higher proportion of TNM stages II and III compared with the PNI-negative group, while PGR was lower. This suggests that PNI is a comprehensive reflection of the highly invasive state of GC. When included in the LASSO regression model, nine indicators with non-zero coefficients were selected. The main reason is that the glycoprotein MUC1 of CA19-9 is associated with glycopeptides on cancer cells, thereby reducing NK cell recognition and cytotoxicity, providing an opportunity for uncontrolled cancer cell growth and migration (Chen *et al*., 2025). Increased tumor thickness leads to intratumoral hypoxia and upregulation of HIF-1α, which enters the nucleus, activates transcription of downstream VEGF genes and promotes angiogenesis, creating conditions for tumor cells to enter perineural lymphatic vessels (Vageli *et al*., 2024). Diffuse-type GC is often characterized by a high frequency of CDH1 mutations, leading to loss-of-function or downregulation of E-cadherin, driving epithelial-mesenchymal transition and a more aggressive tumor cell phenotype (Cerrato-Izaguirre *et al*., 2022). Borrmann type III GC is a malignant tumor with invasive ulceration, usually presenting with a large ulcer surface, which may be related to a stronger local inflammatory response. Studies have shown that in patients with advanced Borrmann type III GC, higher preoperative inflammation levels may promote hematogenous and distant lymph node metastasis by activating the adhesion, proliferation and migration of circulating tumor cells (Wang et al., 2023), thereby increasing PNI risk (Cong *et al*., 2024). Elevated PLR indicates a dual state of pro-inflammation and immunosuppression. In cancer patients, reductions in CD4+ and CD8+ T cells weaken the lymphocyte-dominated antitumor immune response. Platelets not only promote tumor cell proliferation and angiogenesis but also, when activated, further enhance cancer cell growth and survival (Li *et al*., 2023). When the immune system cannot effectively eliminate invasive tumor cell clones, these cells can breach tissue barriers and spread to peripheral structures, such as nerves. Decreased PGR indicates gastric mucosal atrophy, with the typical pathological change being a reduction in the number of gastric glands, leading to decreased gastric acid secretion and, consequently, increased gastric pH (Dondov *et al*., 2022). A low gastric acid environment can lead to gastric flora imbalance, promote nitrosamine synthesis, damage DNA and induce the emergence of more aggressive tumor cell clones (Koga, 2022). Tumor anatomical progression is mainly manifested by deeper invasion, advanced TNM stage and an increased number of lymph node metastases. Increasing tumor invasion depth suggests that tumor invasion has extended from the muscularis propria to the serosa. The muscularis propria and subserosa of the gastric wall are rich in nerve fibers; when tumors progress to this stage, they are more likely

to contact the rich neural network, thus causing PNI. Studies have shown that PNI is associated with tumor stage and invasion depth in GC patients (Ge *et al*., 2024), consistent with our results. It should be noted that CEA, CA125, AFP and CA19-9 were included as candidate predictors based on their routine use in clinical practice for GC and their known associations with tumor biological behavior: CEA reflects tumor burden, CA19-9 is involved in immune evasion and metastatic potential, CA125 indicates serosal invasion and AFP identifies the highly invasive AFP-positive GC subtype.

Results showed that only CA19-9 was significantly elevated in the PNI-positive group and was selected by LASSO into the prediction model, while CEA, CA125 and AFP showed no independent association with PNI. This finding suggests that CA19-9 may contribute to PNI through MUC1-mediated reduction in NK cell recognition and immune evasion (Chen et al., 2025), while the value of traditional markers CEA, CA125 and AFP in PNI prediction is limited. Future studies may focus on CA19-9 or explore more specific neural invasion-related markers. NLR, CRP and other inflammatory markers were not included because platelets play a direct role in tumor-nerve interactions: activated platelets release TGF-β, PDGF and serotonin, which can induce EMT and enhance tumor cell neurotropism, whereas the direct mechanistic links between neutrophils/CRP and PNI remain unclear. In variable selection, LASSO retained PLR as a non-zero coefficient variable, while NLR and CRP showed no independent predictive value. Furthermore, there is a high correlation among inflammatory ratios, such as PLR, NLR and LMR and including them simultaneously may introduce multicollinearity. Future studies may compare the predictive efficacy of different inflammatory markers for PNI.

Significant differences exist between the PNI-positive and PNI-negative groups in serological indicators, tumor anatomical characteristics and histopathological types. These differences reveal multidimensional risk factors for PNI and provide a basis for individualized treatment strategies: before surgery/chemotherapy, PLR and PGR can be measured to identify high-risk PNI patients for early warning; in surgical planning, wider resection margins and more thorough lymph node dissection should be considered for high-risk patients; in adjuvant treatment decisions, PNI-positive patients should receive more intensive chemotherapy regimens and be considered for radiotherapy; in postoperative follow-up, high-risk patients require more frequent monitoring. This comprehensive individualized strategy, spanning from preoperative risk assessment to postoperative follow-up management, has the potential to improve outcomes for high-risk PNI patients while avoiding overtreatment in low-risk patients. It is important to emphasize that although the above mechanisms provide a reasonable explanatory framework for the statistical associations observed in this study, they are derived from the previous literature. This retrospective study did not directly measure expression of related factors or signaling pathways; therefore, these explanations should be considered speculative hypotheses requiring experimental validation in future studies.

Logistic regression analysis showed that PLR and TNM stage were risk factors for PNI in GC patients receiving paclitaxel chemotherapy, while PGR was a protective factor. Thus, PNI is associated with tumor progression and the immune-inflammatory status of GC patients. PLR, as a comprehensive indicator based on peripheral blood platelet and lymphocyte counts, plays an important role in GC prognosis (Peng *et al*., 2022). During cancer progression, tumor cells can enter the peripheral circulation as circulating tumor cells (CTCs) after breaking through mechanical barriers and evading immune surveillance; lymphocytes can directly induce CTC apoptosis and inhibit CTC migration by secreting IFN-γ and TNF-α; upon platelet activation, the release of large amounts of TGF-β and PDGF can activate the Smad and NF-κB pathways and trigger EMT, which further causes tumor cells to lose intercellular connections, thereby significantly enhancing their migration and invasion capabilities and increasing PNI risk (Cong *et al*., 2024). Studies have confirmed that PLR is a significant prognostic factor for GC patients. The 3-year postoperative overall survival rate of the high PLR group was 70.8%, significantly lower than that of the low PLR group (83.6%) (Aoyama *et al*., 2023), consistent with our results. Unlike previous studies, however, our study is the first to focus on the predictive value of PLR for the specific pathological feature of PNI rather than overall survival or recurrence.

Decreased PGR is an important marker reflecting gastric fundic gland atrophy (Ziqi *et al*., 2025). Gastric mucosal atrophy is often accompanied by chronic gastritis, leading to the persistent presence of inflammatory factors such as IL-1β, which can promote GC cell line proliferation through the tyrosine kinase pathway and also activate NF-κB signaling in MDSCs, upregulating IL-6 and TNF-α secretion and indirectly promoting tumor growth. IL-1 can upregulate VEGF levels, thereby improving tumor cell adhesion and promoting metastasis. After activating JAK2/STAT3, IL-6 phosphorylates STAT3, allowing it to enter the nucleus and induce the expression of various oncogenes and transcription factors including c-Fos, TRF-1 and Bcl-2. On one hand, this promotes tumor cell proliferation and differentiation; on the other hand, it also promotes PNI occurrence (Jaroenlapnopparat *et al*., 2022). PLR and PGR have a solid biological basis as predictive biomarkers for PNI. Elevated PLR reflects systemic pro-inflammatory and immunosuppressive imbalance: platelet-released neuroactive substances and

TGF-β enhance tumor cell neurotropism, while lymphopenia weakens immune surveillance. Decreased PGR reflects gastric mucosal atrophy and a local chronic inflammatory microenvironment, producing aggressive tumor clones via the low-acid-dysbiosis-DNA-damage axis and disrupting neural barriers via inflammatory factors. Advanced TNM stage increases the likelihood of physical contact between tumor cells and nerve fibers and indicates that tumors have acquired greater metastatic capacity. These three dimensions provide complementary information and their combined application enables a more comprehensive assessment of PNI risk. These mechanistic hypotheses require further validation through in vitro co-culture systems, animal models and molecular pathological studies of clinical specimens. Studies have shown that a higher TNM stage is a risk factor for poor postoperative prognosis in GC patients (OR=1.909) (Li *et al*., 2026), consistent with our findings. In this study, the apparent AUCs for PLR, PGR, TNM stage and their combined model for predicting PNI were 0.786, 0.807, 0.834 and 0.851, respectively, indicating moderate to good predictive performance (AUC 0.70–0.80: moderate; 0.80–0.90: good). Among single indicators, TNM stage showed the best predictive performance (AUC=0.834), reflecting the strong correlation between anatomical progression and PNI. PGR (AUC=0.807), a preoperatively measurable functional marker, provides information on the gastric mucosal microenvironment not captured by TNM stage. PLR (AUC=0.786) showed relatively lower predictive performance but retains clinical value as a non-invasive, low-cost screening indicator. The combined model showed the best performance (AUC=0.851), indicating that the three indicators provide complementary information across three dimensions—systemic immune-inflammatory status (PLR), local gastric mucosal microenvironment (PGR) and tumor anatomical progression (TNM)—and can comprehensively assess PNI risk, superior to any single indicator. It is important to emphasize that these AUC values reflect apparent performance in the derivation cohort, with inherent optimism bias; true generalizability requires external validation. The optimal cut-off values identified (PLR ≥145.37, TNM stage ≥II, PGR ≤6.12, combined model ≥0.382) provide quantitative references for potential clinical application. These AUC values indicate that each indicator and the combined model exhibit moderate to good discriminatory ability in the derivation cohort. However, an AUC of 0.78–0.85 represents moderate to moderately good performance and cannot yet be considered strong predictive efficacy. Moreover, these results represent apparent performance without external validation and predictive accuracy may decrease in real-world applications. The identified cut-off values provide quantitative references for potential clinical application. For example, PLR ≥145.37 suggests elevated PNI risk (sensitivity 72.5%, specificity 74.8%); such patients may benefit from enhanced pathological detection of PNI in postoperative specimens and closer follow-up. PGR ≤6.12 suggests elevated PNI risk (sensitivity 78.1%, specificity 71.5%); given that decreased PGR reflects gastric mucosal atrophy, such patients might benefit from gastric mucosal protective agents or anti-inflammatory interventions, though this hypothesis requires prospective validation. TNM stage ≥ II has relatively high specificity (76.9%), indicating that patients with advanced stage have a significantly increased PNI risk and that intraoperative pathological assessment of perineural infiltration should receive particular attention. A combined prediction probability ≥0.382, with superior sensitivity (85.6%) and specificity (80.2%) compared with single indicators, is suggested as a clinical warning threshold: patients above this threshold should be considered for targeted pathological detection of postoperative specimens, intensified adjuvant treatment decisions and closer recurrence monitoring. It must be emphasized, however, that these cut-off values and corresponding sensitivity/specificity estimates are derived from single-center retrospective data and carry a risk of overfitting. Therefore, before external validation, these cut-off values should not be used as rigid thresholds for clinical decisions but rather regarded as preliminary references for risk stratification. Calibration curve analysis showed good clinical calibration of the combined prediction model and the DCA curve indicated favorable clinical net benefit within the 0%–71% threshold range.

Spearman analysis showed that PGR was negatively correlated with PNI (r = -0.749, -0.698,- 0.751), whereas PLR and TNM stage were positively correlated. This further indicates that PLR, TNM stage and PGR can help identify high-risk individuals for PNI, providing a reference for clinical treatment. This study found that PLR and PGR were significantly associated with PNI, suggesting that these factors may serve as potential intervention targets to reduce PNI risk. However, there is currently no direct evidence that anti-inflammatory therapy or interventions to reduce gastric mucosal atrophy can reduce PNI risk in GC patients. Future studies may explore: (1) in prospective cohort studies, whether PNI incidence is reduced in GC patients using aspirin or statins; (2) whether PNI risk decreases synchronously in patients with PGR improvement after H. pylori eradication; (3) in animal models, the causal effect of anti-inflammatory therapy on PNI occurrence. Such studies would provide a theoretical basis for chemoprevention of PNI.

Nevertheless, this study has several limitations. First, as a single-center retrospective study, selection bias may exist; all predictive performance metrics reflect apparent performance based on the derivation cohort, with optimism bias due to overfitting and the model has not been externally validated, so its generalizability remains unclear. Second, the sample size is relatively small;

although it meets the basic EPV≥10 requirement, statistical power is limited. Third, the mechanistic interpretations presented in the discussion are derived from previous literature; this study did not measure cytokines, signaling pathway molecules, or immune cell subsets, so all mechanistic discussions should be considered exploratory hypotheses. Fourth, this study did not include overall survival or progression-free survival as endpoints. Fifth, the reported cut-off values are derived from the cohort and are sensitive to sample distribution, requiring recalibration in external validation. Therefore, the results of this study should be considered exploratory, hypothesis-generating, preliminary findings. Future multicenter prospective studies with external validation and long-term follow-up data are needed to assess the model's indirect predictive value for survival outcomes.

CONCLUSION

In summary, based on apparent performance analysis of a single-center derivation cohort, PGR and PLR show moderate predictive value for post-chemotherapy PNI status in GC patients, with slightly improved combined predictive performance when TNM stage is added. However, all mechanistic explanations are speculative hypotheses based on previous literature and all predictive performance metrics represent apparent performance. External validation is required before clinical value can be properly assessed.

Acknowledgments
We gratefully acknowledge the Natural Science Foundation of Fujian Province (2024J011470).

Author's contributions
Yongliang Li: Conceptualization, Methodology, Writing – original draft; Xi Lin: Data curation, Formal analysis and Investigation; Guofeng Lin: Validation, Visualization and Writing – review & editing; Feiteng Gu: Project administration and Funding acquisition. The author read and approved the final manuscript.

Funding
This work was supported by the Natural Science Foundation of Fujian Province (Grant No. 2024J011470), awarded to Dr. Yongliang Li. The funder had no role in the study design, data collection, data analysis, data interpretation, manuscript preparation, or the decision to submit the manuscript for publication. The funder provided financial support solely for the conduct of the research and the publication of the results. All authors had full access to all study data and take full responsibility for the integrity of the data and the accuracy of the data analysis.

Data availability statement
All data generated or analyzed during this study are included in this published article and its supplementary information files.

Ethical approval
This study was approved by the ethics committee of Affiliated Hospital of Putian University (NO. 2025698). This study was performed in adherence with the STROBE guidelines. See supplementary file for the STROBE checklist.

Conflict of interest
The authors declare that this study was conducted in the absence of any commercial or financial relationships that could be construed as a potential conflict of interest.

REFERENCES

Aoyama T, Hashimoto I, Maezawa Y, Hara K, Kazama K, Numata M, Kamiya N, Tamagawa H, Sawazaki S, Kawahara S, Komori K, Tamagawa A, Cho H, Morita J, Otani K, Kato A, Tanabe M, Oshima T, Yukawa N, Saito A and Rino Y (2023). The clinical impact of the pretreatment platelet-to-lymphocyte ratio in gastric cancer patients who receive curative treatment. *In Vivo*., **37**(6): 2696-2703.

Cao M, Hu C, Pan S, Zhang Y, Yu P, Zhang R, Cheng X and Xu Z (2024). Development and validation of nomogram for predicting early recurrence after radical gastrectomy of gastric cancer. *World J Surg Oncol*., **22**(1): 21.

Cerrato-Izaguirre D, Chirino YI, Prada D, Quezada-Maldonado EM, Herrera LA, Hernandez-Guerrero A, Alonso-Larraga JO, Herrera-Goepfert R, Onate-Ocana LF, Cantu-de-Leon D, Meneses-Garcia A, Basurto-Lozada P, Robles-Espinoza CD, Camacho J, García-Cuellar CM and Sanchez-Perez Y (2022). Somatic mutational landscape in Mexican patients: Cdh1 mutations and Chr20q13.33 amplifications are associated with diffuse-type gastric adenocarcinoma. *Int J Mol Sci*., **23**(19):11116.

Chen YF, Wang SY, Le PH, Chen TH, Kuo CJ, Lin CJ, Chou WC, Yeh TS and Hsu JT (2022). Prognostic significance of perineural invasion in patients with stage Ii/Iii gastric cancer undergoing radical surgery. *J Pers Med*., **12**(6): 962.

Chen C, Patel A, Demirkhanyan L and Gondi CS (2025). The role of mucins in cancer and cancer progression: A comprehensive review. *Curr Issues Mol Biol*., **47**(6): 406.

Cong R, Xu R, Ming J and Zhu Z (2024). Construction of a preoperative nomogram model for predicting perineural invasion in advanced gastric cancer. *Front Med (Lausanne)*., **11**:1344982.

Dondov G, Amarbayasgalan D, Batsaikhan B, Badamjav T, Batbaatar B, Tuvdenjamts B, Tumurbat N, Davaa B, Purevdorj E, Nyamaa B and Lonjid T (2022). Diagnostic performances of pepsinogens and gastrin-17 for atrophic gastritis and gastric cancer in mongolian subjects. *PLoS One*., **17**(10): e0274938.

Gangannapalle M, Shahnoor H, Sattar L, Nagi TK, Al-

Article in Press

Tekreeti M, Khan MW, Haseeb MD and Khan A (2023). Nanoparticle albumin-bound paclitaxel and solvent-based paclitaxel as chemotherapy options for patients with advanced gastric cancer: A systematic review and meta-analysis. *Cureus*., **15**(7): e41711.

Ge HT, Chen JW, Wang LL, Zou TX, Zheng B, Liu YF, Xue YJ and Lin WW (2024). Preoperative prediction of lymphovascular and perineural invasion in gastric cancer using spectral computed tomography imaging and machine learning. *World J Gastroenterol*., **30**(6): 542-555.

Huang P, Li S, Deng Z, Hu F, Jin D, Xiong S and Fan B (2025). Machine-learning based computed tomography radiomics nomgram for predicting perineural invasion in gastric cancer. *Curr Med Imaging*., **21**: e15734056323323.

Jaroenlapnopparat A, Bhatia K and Coban S (2022). Inflammation and gastric cancer. *Diseases*., **10**(3): 35.

Koga Y (2022). Microbiota in the stomach and application of probiotics to gastroduodenal diseases. *World J Gastroentero*l., **28**(47): 6702-6715.

Li C, Wang M, Cheng X, Jiang Y and Xiao H (2022). Nerve invasion as an independent predictor of poor prognosis in gastric cancer after curative resection. *Medicine (Baltimore)*., **101**(33): e30084.

Li B, Wang K, Shi S, Li M, Ma MT, Zhou ZG, Wang ZC, Gong YN, Xiao Y, Zhao L, Meng Q and Liu YB (2023). Prognostic value of neutrophil to lymphocyte ratio and platelet counts during chemotherapy in patients with advanced gastric cancer. *Saudi Med J*., **44**(11): 1104-1112.

Li H, Li N, Zhu D, Hou S, Chang Y, Duan Q, Wu J and Yin J (2026). Critical perioperative factors influencing postoperative complications and long-term survival in patients with gastric cancer. *JSLS*., **30**(1): e2025.00123.

Nasier-Hussain M, Samanje JN, Mokhtari K, Nabi-Afjadi M, Fathi Z, Hoseini A and Bahreini E (2025). Serum levels of oxidative stress, Il-8 and pepsinogen i/Ii ratio in helicobacter pylori and gastric cancer patients: Potential diagnostic biomarkers. *BMC Gastroenterol*., **25**(1): 2.

Liebig C, Ayala G, Wilks JA, Berger DH and Albo D (2009). Perineural invasion in cancer: a review of the literature. *Cancer*., **115**(15): 3379-3391.

Özcan P and Çarkman MS (2024). The relationship between the prognostic nutritional index and lymphovascular and perineural invasion of the tumor in patients diagnosed with gastric cancer and its effect on overall survival. *Medicine (Baltimore)*., **103**(42): e40087.

Park S, Kim YH, Bang HI and Park Y (2023). Sample size calculation in clinical trial using R. *J Minim Invasive Surg*., **26**(1): 9-18.

Peng X, Zeng W, Tang B, He A, Zhang M and Luo R (2022). Utility of pretreatment blood platelet-to-lymphocyte ratio in prediction of clinical outcomes and chemosensitivity in patients with advanced gastric cancer: A meta-analysis. *Med Sci Monit*., **28**: e933449.

Petrova V, Mills CE, Hug C, Cetinkaya-Fisgin A, Splaine J, Fouladzadeh S, Hakim S, Powell R, Zhen S, Chung M, Bradshaw GA, Deng T, Singec I, Wang Q, Kawaguchi R, Jonnagaddala H, Barrett LB, Smith JA, Kalocsay M, Gyori BM, Hoke A, Sorger PK and Woolf CJ (2026). A human iPSC-derived sensory neuron platform for high-throughput discovery of neuroprotectants against chemotherapy-induced peripheral neuropathy. *Cell Rep Med*., **7**(5): 102787.

Sohrab SS, Raj R, Nagar A, Hawthorne S, Paiva-Santos AC, Kamal MA, El-Daly MM, Azhar EI and Sharma A (2023). Chronic inflammation's transformation to cancer: A nanotherapeutic paradigm. *molecules*., **28**(11): 4413.

Tan S, Zheng Q, Zhang W, Zhou M, Xia C and Feng W (2024). Prognostic value of inflammatory markers Nlr, Plr and Lmr in gastric cancer patients treated with immune checkpoint inhibitors: A meta-analysis and systematic review. *Front Immunol*., **15**: 1408700.

Vageli DP, Doukas PG, Goupou K, Benos AD, Astara K, Zacharouli K, Sotiriou S and Ioannou M (2024). Hypoxia-inducible factor 1alpha and vascular endothelial growth factor in glioblastoma multiforme: A systematic review going beyond pathologic implications. *Oncol Res*., **32**(8): 1239-1256.

Wang J, Feng F, Du K, Yang X, Liu S, Xu C, Li M, Tan Z, Li X, Wang S, Yang X, Li S, Yu P, Wei J, Xu G, Hong L, Zheng J and Yang J (2025). Main results of a randomized controlled trial (Rnpls-01): Efficacy and safety of ramucirumab combined with nab-paclitaxel, lobaplatin and s-1 in neoadjuvant therapy for advanced gastric cancer. *Int J Surg*., **111**(11): 8060-8069.

Wang H, Yin X, Ma K, Wang Y, Fang T, Zhang Y and Xue Y (2023). Nomogram based on preoperative fibrinogen and systemic immune-inflammation index predicting recurrence and prognosis of patients with borrmann type Iii advanced gastric cancer. *J. Inflamm. Res*., **16**:1059-1075.

Zhang F, Chen H, Luo D, Xiong Z, Li X, Yin S, Jin L, Chen S, Peng J and Lian L (2023). Lymphovascular or perineural invasion is associated with lymph node metastasis and survival outcomes in patients with gastric cancer. *Cancer Med*., **12**(8):9401-9408.

Ziqi C, Xin D, Temuribagen, Caimeng XU, Shaonan HU, Qianwen C, Yuewu W, Haibo W, Xiaoyu HE, Dan X and Peifeng X (2025). Exploration of the mechanism of the mongolian medicine tonglaga-5 (-5) For the treatment of n-Methyl-n'-Nitro-n-Nitrosoguanidine-induced chronic atrophic gastritis based on network pharmacology and metabolomics. *J Tradit Chin Med*., **45**(6): 1366-1375.